ANN- Controlled Three Phase Bi-directional EV Battery Charger for G2V & V2G Operation with Improved Grid Power Quality

Janagani Yashwanth Kumar[1], Thota Rajesh[2*]
[1]PG Student, [2]Assistant Professor, [1,2]Department of Electrical and Electronics Engineering
[1,2]Vaagdevi College of Engineering (UGC-Autonomous), Bollikunta, Warangal, 506005, Telangana
[1]yashwanthjanagani123@gmail.com, [2]rajesh_t@vaagdevi.edu.in
*Correspondence: Thota Rajesh(rajesh_t@vaagdevi.edu.in)

ABSTRACT

Global electric vehicle (EV) adoption continues to increase rapidly, with worldwide EV sales exceeding 17 million units in 2024, while EVs accounted for more than 20% of new car sales globally, highlighting the growing demand for intelligent bidirectional charging infrastructures. The rapid expansion of smart grids and renewable energy integration has further accelerated the need for efficient Vehicle-to-Grid (V2G) and Grid-to-Vehicle (G2V) technologies capable of supporting grid stability and sustainable energy management. Bidirectional EV chargers are increasingly required in residential, commercial, and public charging stations to enable peak load management, renewable energy utilization, emergency backup power, and grid ancillary services. These applications demand fast dynamic response, accurate power regulation, and reliable bidirectional energy transfer under varying operating conditions. However, conventional proportional-integral (PI) controller-based chargers suffer from fixed controller gains, slower transient response, limited adaptability to nonlinear system dynamics, increased steady-state error, and reduced performance under fluctuating grid and battery conditions. To overcome these limitations, this paper proposes an Artificial Neural Network (ANN)-based bidirectional battery charger for intelligent G2V and V2G operation. The proposed architecture integrates a three-phase isolation transformer, LCL filter, bidirectional AC/DC converter, DC-link capacitor, bidirectional DC/DC converter, output filter, Energy Management System (EMS), and ANN-based voltage and current controllers. Real-time measurements of grid voltage, current, frequency, battery voltage, battery current, state-of-charge (SoC), and DC-link voltage are processed by the ANN to generate adaptive PWM control signals for both converters. The proposed intelligent controller achieves accurate DC-link voltage regulation, superior current tracking, improved converter efficiency, reduced harmonic distortion, enhanced power quality, faster dynamic response, and reliable bidirectional energy transfer, making it well suited for next-generation smart-grid-integrated EV charging applications.

Keywords: Artificial Neural Network (ANN), Bidirectional Battery Charger, Electric Vehicle (EV), Grid-to-Vehicle (G2V), Vehicle-to-Grid (V2G), Energy Management System (EMS).

1. INTRODUCTION

The evolution of smart grids has further strengthened the importance of intelligent EV charging technologies. Unlike conventional charging systems that only draw power from the utility grid, bidirectional charging systems enable electricity to flow in both directions, allowing batteries to be charged during low-demand periods and discharged during peak demand conditions. This capability improves energy utilization, reduces stress on utility infrastructure, and enhances overall grid reliability. Moreover, bidirectional charging supports applications such as peak shaving, load balancing, voltage regulation, renewable energy integration, and emergency backup power. As EV adoption continues to increase globally, charging systems are expected to operate efficiently under highly dynamic operating conditions involving fluctuating grid voltage, varying battery state-of-charge, and continuously changing load demand. Therefore, intelligent and reliable charging infrastructures have become an essential component of future smart energy ecosystems.

Figure 1.1 illustrates the projected growth of the Indian electric vehicle (EV) market from 2020 to 2030, categorized into Battery Electric Vehicles (BEVs) and Plug-in Hybrid Electric Vehicles (PHEVs), with market size represented in billions of U.S. dollars (USD). The figure indicates a steady increase in market value during the early years from 2020 to 2024, reaching approximately USD 8.5 billion in 2024. From 2025 onward, the market exhibits accelerated expansion, driven by increasing EV adoption, government incentives, advancements in battery technology, expansion of charging infrastructure, and growing consumer awareness regarding sustainable transportation. The market is forecast to grow at a Compound Annual Growth Rate (CAGR) of 40.7% during the period 2025–2030, demonstrating one of the fastest-growing EV markets globally. Battery Electric Vehicles (BEVs) constitute the dominant share of the market throughout the forecast period due to their zero-emission operation, lower maintenance requirements, and continuous improvements in battery performance and driving range, while Plug-in Hybrid Electric Vehicles (PHEVs) contribute an additional share by providing flexible operation through combined electric and internal combustion propulsion. The projected market expansion also reflects increasing investments by automobile manufacturers, battery producers, charging infrastructure providers, and renewable energy companies. Furthermore, the rapid growth of the EV market is expected to increase electricity demand and create a greater need for efficient smart charging systems capable of supporting bidirectional energy transfer, grid stability, renewable energy integration, and intelligent energy management.

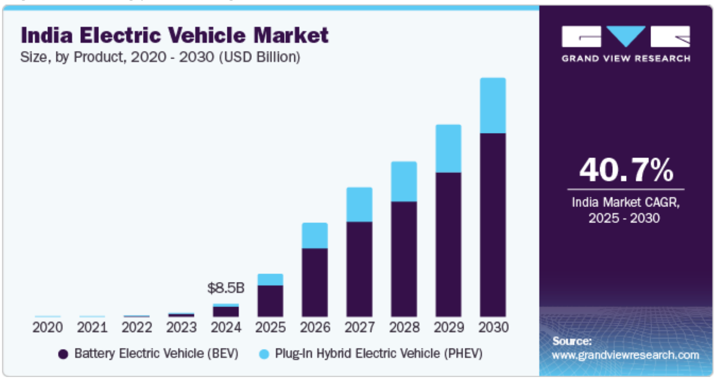

Figure 1. India Electric Vehicle Market Growth Forecast (2020–2030).

(Source: https://www.grandviewresearch.com/industry-analysis/india-electric-vehicle-market-report)

1.2 Research Objectives

- To analyze the performance limitations of conventional PI controller-based bidirectional EV battery charging systems operating in Grid-to-Vehicle (G2V) and Vehicle-to-Grid (V2G) modes.
- To develop an Artificial Neural Network (ANN)-based intelligent control framework for adaptive DC-link voltage regulation, current control, and bidirectional power flow management.
- To improve converter efficiency, power quality, dynamic response, harmonic suppression, and reliable energy exchange between electric vehicles and the smart grid using intelligent ANN-based control.

2. LITERATURE SURVEY

Pinto et al. [1] introduced a multifunctional on-board charger for electric vehicles that supports bidirectional energy exchange through Grid-to-Vehicle (G2V), Vehicle-to-Grid (V2G), and Vehicle-to-Home (V2H) operating modes. The developed charger enables battery charging with a near-unity power factor while also allowing stored battery energy to be delivered either to the utility grid or household loads. A dedicated control mechanism was implemented to ensure seamless transitions between charging and discharging operations while maintaining stable voltage and current characteristics. In addition, an optimized passive filter on the AC side effectively reduced harmonic distortion, thereby improving overall power quality. Both simulation and hardware validation verified reliable bidirectional power transfer and demonstrated the suitability of the charger for smart-grid-based EV applications. Zgheib et al. [2] developed a bidirectional battery charging system for electric vehicles based on a cascaded Model Predictive Control (MPC) framework supporting G2V, V2G, and Vehicle-for-Grid (V4G) functionalities. The proposed control strategy independently regulated active and reactive power exchanged with the grid while simultaneously maintaining precise battery current control. Through the V4G operating mode, the charger was capable of supplying reactive power compensation alongside battery charging or discharging to improve voltage stability within the electrical network. The system provided four-quadrant power flow capability, enabling flexible energy management. Experimental investigations and simulation studies confirmed accurate power tracking, fast transient response, and stable converter operation under different loading conditions.

Chakraborty et al. [3] presented a comprehensive review of bidirectional DC–DC converter configurations employed in battery electric vehicles, plug-in hybrid electric vehicles, and high-power charging stations. Various converter topologies were evaluated considering performance indicators such as conversion efficiency, electromagnetic interference, reliability, implementation cost, and current ripple. Among the investigated structures, the Multidevice Interleaved Bidirectional DC–DC Converter (MDIBC) was identified as a promising solution for high-power charging applications because of its superior efficiency and reduced ripple characteristics. The study also highlighted the growing importance of silicon carbide (SiC) and gallium nitride (GaN) semiconductor devices for future converter development and emphasized the need for advanced converter architectures and intelligent control techniques. Koushki et al. [4] conducted a detailed review of bidirectional AC–DC converter topologies designed for on-board EV chargers with Vehicle-to-Grid capability. The comparison included both isolated and non-isolated converter structures evaluated in terms of conversion efficiency, switching losses, power factor correction, reliability, implementation complexity, and safety requirements. The authors reported that active power factor correction methods significantly enhanced power quality while minimizing harmonic injection into the utility grid. The study concluded that selecting an appropriate converter topology depends on the intended application, converter power rating, and operational constraints.

Nema et al. [5] surveyed the latest developments in wireless Battery Management Systems (wBMS) for electric vehicles and compared their performance with conventional wired battery management architectures. The review highlighted that wireless systems substantially reduce cable complexity, decrease vehicle weight, simplify maintenance procedures, and provide greater design flexibility. Different wireless communication protocols were examined with respect to reliability, latency, communication quality, and implementation feasibility. The authors also discussed challenges including cybersecurity, electromagnetic interference, communication delays, and power consumption, identifying these issues as key research directions before large-scale industrial deployment becomes feasible. Kumar and Ojha [6] investigated the design methodology of an electric rickshaw incorporating regenerative braking to improve overall energy utilization. The proposed vehicle architecture integrated the regenerative braking mechanism with the electric motor, controller, battery pack, and associated power electronic circuitry to recover kinetic energy during vehicle deceleration. The recovered energy was redirected to recharge the battery, thereby increasing driving range while reducing overall energy losses. The study demonstrated improvements in battery life, vehicle efficiency, and operating economy, providing practical design recommendations for future electric rickshaw development.

Kumar and Ojha [7] reviewed recent technological progress in electric vehicles intended for urban and local transportation systems. The investigation covered charging technologies, battery chemistries, charging infrastructure, and energy storage solutions currently employed in modern EVs. The authors discussed existing limitations related to long charging durations, limited driving range, and customer convenience while emphasizing the importance of efficient charging strategies and advanced battery management techniques. The review concluded that continuous innovations in battery technology and charging infrastructure will play a vital role in accelerating EV adoption. Ojha et al. [8] examined carrier-based pulse-width modulation techniques for minimizing common-mode voltage in neutral-point-clamped (NPC) inverter-based AC–DC–AC drive systems. Multiple PWM strategies were analyzed to reduce leakage current and electromagnetic interference without introducing additional hardware components. The proposed modulation approaches successfully lowered common-mode voltage while preserving output voltage quality and inverter performance. Validation through simulation and experimental implementation demonstrated enhanced drive reliability and improved operating efficiency for NPC inverter systems.

Viswanatha et al. [9] reviewed recent developments in bidirectional DC–DC converter topologies and intelligent control techniques for electric vehicles, renewable energy integration, and DC microgrid applications. Different converter structures were comparatively analyzed based on voltage regulation capability, conversion efficiency, bidirectional power flow, implementation complexity, and overall performance. The review further evaluated several advanced control algorithms, including proportional-integral-derivative (PID), fuzzy logic, neural networks, and sliding mode control. The authors concluded that intelligent control strategies significantly improve converter stability, dynamic response, and energy conversion efficiency compared with conventional control approaches. Viswanatha et al. [10] proposed an average large-signal state-space modeling methodology for DC–DC buck converters to derive transfer function models suitable for closed-loop controller design. Both conventional PID and PID with filter coefficient (PIDN) controllers were developed for analog and digital voltage-mode control applications. Frequency-domain characteristics were investigated using Bode plots and pole-zero analysis, while performance evaluation was carried out through simulation in Simulink and a computational modeling environment. The results demonstrated that the PIDN controller achieved faster transient response, increased bandwidth, improved gain characteristics, and better steady-state regulation than the conventional PID controller. Furthermore, optimization of the filter coefficient effectively suppressed high-frequency disturbances and reduced control signal oscillations, demonstrating the practicality of the proposed controller for DSP- and FPGA-based embedded converter implementations.

Ashwini Kumari and Geethanjali [11] carried out an extensive review of parameter extraction methods used in photovoltaic (PV) systems operating under both uniform irradiance and partial shading conditions. The survey classified existing techniques into analytical, numerical, and evolutionary optimization approaches and assessed their effectiveness in estimating PV model parameters for enhanced energy conversion and maximum power point tracking (MPPT). The authors observed that conventional analytical and iterative methods often encounter challenges related to convergence, singularity, and sensitivity to environmental variations. In contrast, metaheuristic optimization algorithms, including Genetic Algorithm (GA), Particle Swarm Optimization (PSO), and Differential Evolution (DE), provided more reliable parameter estimation with improved accuracy. The review concluded that combining multi-objective optimization strategies with robust MPPT techniques can significantly improve photovoltaic system performance under dynamically changing weather conditions. Dominguez et al. [12] proposed a cascade-based Sliding Mode Control (SMC) technique operating at a fixed switching frequency for a half-bridge bidirectional DC–DC converter designed for electric traction systems. A small-signal averaged state-space model was first established to support the controller design and validate the cascade control configuration. The proposed sliding mode controller was then evaluated under multiple operating conditions and benchmarked against a conventional single-loop SMC approach. Simulation studies demonstrated that the cascade controller achieved faster transient characteristics, more accurate voltage regulation, and stronger robustness against parameter uncertainties and load variations. The investigation confirmed that the proposed control scheme is highly effective for improving the dynamic performance of bidirectional converters employed in electric vehicle applications.

Tahim et al. [13] introduced a nonlinear control methodology for bidirectional DC–DC converters operating within standalone DC microgrids. The proposed controller was designed to regulate the DC bus voltage while facilitating smooth bidirectional power transfer between the battery energy storage system and the microgrid. The nonlinear control algorithm maintained stable converter operation despite system disturbances, load fluctuations, and component parameter variations. Performance evaluation through simulation revealed superior voltage regulation, faster transient recovery, and improved disturbance rejection compared with conventional linear controllers. The authors concluded that the proposed nonlinear control strategy enhances converter reliability and overall operational stability in standalone DC microgrid environments. Aravkin et al. [14] investigated Bayesian hyperparameter estimation techniques for linear system identification using an empirical Bayes framework. The study incorporated stability-aware prior distributions together with tunable hyperparameters to improve the adaptability and estimation capability of Bayesian identification models. Two estimation approaches, namely Maximum Marginal Likelihood (MML) and Minimum Mean Squared Error (MMSE), were comparatively analyzed under simplified identification scenarios. Experimental results demonstrated that accurate hyperparameter optimization substantially improved model estimation accuracy while preserving the stability characteristics of the identified dynamic systems. The research established empirical Bayes estimation as a robust methodology for enhancing the reliability and precision of linear system identification.

3. PROPOSED SYSTEM

Despite providing reliable bidirectional charging functionality, the existing system exhibits several operational limitations when subjected to rapidly changing grid and battery conditions. Conventional PI controllers employ fixed control parameters that cannot adapt automatically to nonlinear system dynamics, resulting in slower transient response, increased steady-state error, and reduced control accuracy. The charger experiences difficulty in maintaining stable DC-link voltage and precise current regulation during abrupt changes in charging demand or grid disturbances. Furthermore, limited intelligent decision-making capability restricts real-time optimization of power flow, battery utilization, and energy management. These shortcomings reduce converter efficiency, increase harmonic distortion under dynamic conditions, and limit the overall performance of the bidirectional charging system in advanced smart-grid environments.

Figure 2 illustrates the proposed ANN-based bidirectional battery charger architecture for EV applications operating in both G2V and V2G modes. The proposed system comprises a three-phase utility grid, an isolation transformer, a bidirectional AC/DC converter, a DC-link capacitor, a bidirectional DC/DC converter with an output filter, an EV battery, measurement units, an ANN controller, converter control logic, and an EMS. The ANN controller receives real-time information from the grid, battery, and converter through multiple measurement units, including grid voltage, current, frequency, battery voltage, battery current, SoC, and DC-link voltage. Based on these operating conditions and EMS commands, the ANN predicts the optimal converter operating mode and generates appropriate PWM switching signals through the converter control logic. Consequently, the proposed intelligent control system enables efficient bidirectional power transfer, accurate battery charging and discharging, improved power quality, enhanced converter efficiency, reduced harmonic distortion, and reliable operation under varying grid and battery conditions.

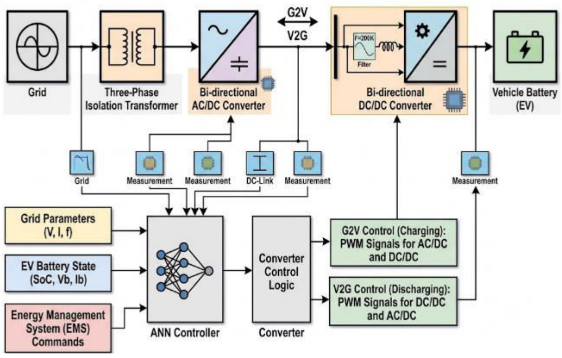

Figure 2. Proposed system architecture.

3.1 Three-Phase Bi-Directional Battery Charger

Figure 3 illustrates the circuit configuration of a three-phase bidirectional battery charger designed for EV applications. The charger consists of a three-phase AC grid interface, an LCL filter, a three-phase bidirectional AC/DC converter, a DC-link capacitor, a bidirectional DC/DC converter, an output filter, and a battery energy storage system. The AC/DC converter is formed by six power semiconductor switches arranged in a three-phase voltage source converter (VSC) configuration, enabling bidirectional power flow between the utility grid and the battery. The DC-link capacitor stabilizes the intermediate DC voltage, while the bidirectional DC/DC converter regulates battery charging and discharging currents. This topology supports Grid-to-Vehicle (G2V), Vehicle-to-Grid (V2G), and Vehicle-to-Load (V2L) operations with improved power quality, reduced harmonic distortion, and high conversion efficiency.

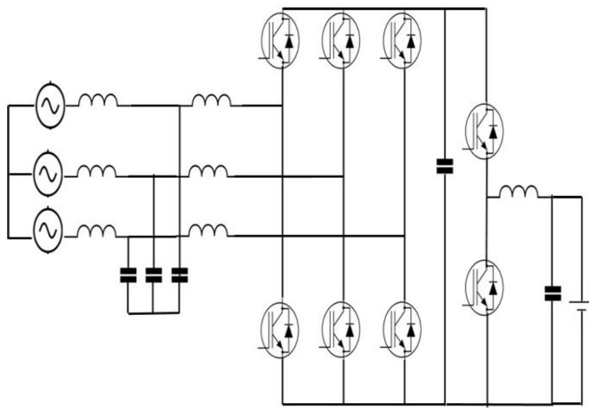

Figure 3: Circuit Diagram of Three-Phase Bi-Directional Battery Charger

The integrated operation of the three-phase AC supply, LCL filter, bidirectional AC/DC converter, DC-link capacitor, bidirectional DC/DC converter, and battery storage system enables efficient bidirectional energy transfer. The charger provides high power density, fast charging capability, grid support functionality, improved power quality, and reliable operation for modern electric vehicle applications supporting G2V, V2G, and V2L services.

3.2 LCL Filter

Figure 4 illustrates the LCL filter employed between the AC grid and the power converter in the bidirectional EV charger system. The filter consists of a grid-side inductor, a converter-side inductor, and a shunt capacitor connected between them. The source voltage represents the utility grid, while the converter denotes the bidirectional AC/DC power conversion stage. The primary function of the LCL filter is to attenuate high-frequency switching harmonics generated by the converter before they are injected into the grid. Compared with conventional L-filters, the LCL filter provides superior harmonic suppression with smaller inductance values, resulting in reduced system size, lower power losses, and improved power quality. The filter also helps maintain a near-sinusoidal grid current and supports compliance with grid interconnection standards.

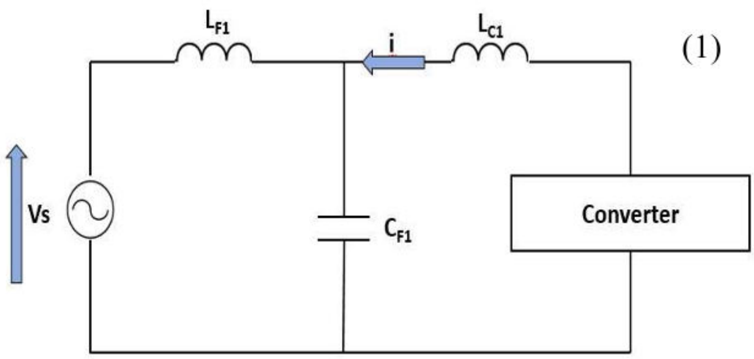

(1)

Figure 4. LCL Filter

3.3 Proposed ANN Control System

Figure 5 illustrates the proposed ANN based control system developed for the bidirectional electric vehicle charger operating in both G2V and V2G modes. The proposed controller integrates three intelligent control loops, namely the ANN DC voltage controller, ANN current controller, and ANN-based converter controller, to regulate the DC-link voltage, grid current, and inverter switching signals simultaneously. The measured three-phase grid voltages and currents are transformed from the stationary abcreference frame into the synchronous rotating dqreference frame using Clarke and Park transformations synchronized by the Phase-Locked Loop (PLL). The ANN controllers replace conventional PI controllers for voltage and current regulation, enabling adaptive learning of nonlinear system dynamics and rapid response under varying grid and battery conditions. The generated reference voltages are converted into PWM switching pulses that control the inverter while the LCL filter suppresses switching harmonics before power exchange with the utility grid. Consequently, the proposed intelligent control system provides superior dynamic response, accurate DC-link voltage regulation, reduced harmonic distortion, and improved bidirectional power transfer efficiency.

Grid Voltage Measurement and Synchronization: The operation begins by continuously measuring the three-phase grid voltages V_a, V_b, and V_c, collectively represented as V_{abc}. These voltages are first transformed into the stationary reference frame using the Clarke transformation to obtain the orthogonal voltage components $V_\alpha$and V_β. The transformed voltages are then supplied to the Phase-Locked Loop (PLL), which estimates the instantaneous grid angle $\theta = \omega t$. The estimated angle is continuously updated and used to synchronize all subsequent coordinate transformations. The Clarke transformation is expressed as

$$\begin{bmatrix} V_\alpha \\ V_\beta \end{bmatrix} = \frac{2}{3}\begin{bmatrix} 1 & -\frac{1}{2} & -\frac{1}{2} \\ 0 & \frac{\sqrt{3}}{2} & -\frac{\sqrt{3}}{2} \end{bmatrix}\begin{bmatrix} V_a \\ V_b \\ V_c \end{bmatrix} \tag{3.1}$$

where V_a, V_b, and V_c denote the measured three-phase grid voltages, while V_α and V_β represent the stationary orthogonal voltage components.

Grid Current Transformation: The three-phase grid currents I_a, I_b, and I_c are measured and transformed into stationary coordinates $I_\alpha$and I_β. Subsequently, the Park transformation converts these stationary currents into synchronous dq-axis currents $I_d$and $I_q$using the PLL angle θ. The direct-axis current $I_d$controls active power transfer, whereas the quadrature-axis current $I_q$regulates reactive power exchange with the utility grid. The Park transformation is written as

$$\begin{bmatrix} I_d \\ I_q \end{bmatrix} = \begin{bmatrix} \cos\theta & \sin\theta \\ -\sin\theta & \cos\theta \end{bmatrix}\begin{bmatrix} I_\alpha \\ I_\beta \end{bmatrix} \tag{3.2}$$

where $I_d$and $I_q$denote the synchronous current components responsible for active and reactive power regulation, respectively.

ANN DC-Link Voltage Controller: The DC-link voltage $V_{DC}$is continuously monitored and compared with its reference value V_{DCref}. The resulting voltage error becomes the input to the ANN DC voltage controller instead of a conventional PI controller. The ANN predicts the appropriate active current reference $I_{dref}$by learning the nonlinear relationship between voltage deviation and converter dynamics. The voltage error is computed as

$$e_v = V_{DCref} - V_{DC} \tag{3.3}$$

where $V_{DCref}$is the desired DC-link voltage, $V_{DC}$is the measured DC-link voltage, and $e_v$represents the voltage regulation error used as the ANN input for adaptive voltage stabilization.

ANN Active Current Reference Generation: The ANN voltage controller processes the voltage error using interconnected neurons with adaptive weights and nonlinear activation functions to generate the desired direct-axis current reference I_{dref}. Unlike fixed-gain PI controllers, the ANN continuously updates its output according to operating conditions, ensuring rapid voltage recovery during disturbances. The ANN neuron output is represented as

$$I_{dref} = f(\sum_{i=1}^{n} w_i\, x_i + b) \tag{3.4}$$

where x_i denotes the ANN input variables, w_i represents synaptic weights, b is the neuron bias, and $f(\cdot)$ is the nonlinear activation function producing the reference current.

Reactive Current Reference: The proposed controller maintains unity power factor by setting the quadrature-axis reference current equal to zero throughout normal operation. This prevents unnecessary reactive power exchange with the utility grid while maximizing converter efficiency. Therefore, $I_{qref} = 0$, where I_{qref} represents the reactive current reference. By forcing I_q toward zero, the grid current remains aligned with the grid voltage, thereby maintaining unity power factor and minimizing reactive power losses.

ANN-Based Current Controller: The measured current components I_d and I_q are compared with their reference values I_{dref} and I_{qref}. The resulting current errors are supplied to the ANN current controller, which estimates the required control voltages U_d and U_q. The ANN effectively compensates for nonlinear converter characteristics and parameter variations while providing faster transient response than conventional controllers. The current errors are

$$e_d = I_{dref} - I_d \tag{3.5}$$

$$e_q = I_{qref} - I_q \tag{3.6}$$

where e_d and e_q denote the direct-axis and quadrature-axis current errors, respectively.

Cross-Coupling Compensation: The converter exhibits coupling between the d-axis and q-axis current dynamics due to the rotating reference frame. Therefore, cross-coupling compensation is introduced to improve current regulation accuracy. The compensated voltage commands are obtained as

$$E_d = U_d + V_d + \omega L I_q \tag{3.7}$$

$$E_q = U_q + V_q - \omega L I_d \tag{3.8}$$

where V_d and V_q are the grid voltage components, L is the filter inductance, ω is the electrical angular frequency, and E_d and E_q are the compensated voltage references.

Voltage Reference Generation: The compensated voltages are normalized with respect to the measured DC-link voltage to generate inverter modulation signals. These normalized quantities determine the required modulation index and switching duty ratio for the inverter. The normalization equation is

$$M_d = \frac{2E_d}{V_{DC}}, M_q = \frac{2E_q}{V_{DC}} \tag{3.9}$$

where M_d and M_q represent the normalized modulation signals and V_{DC} is the measured DC-link voltage.

Inverse Coordinate Transformation: The normalized voltage references are transformed from the synchronous dq reference frame back into the stationary $\alpha\beta$ frame and finally into the three-phase abc reference frame. These reference voltages determine the desired inverter output waveform synchronized with the utility grid. The inverse Park transformation is expressed as

$$\begin{bmatrix} V_\alpha \\ V_\beta \end{bmatrix} = \begin{bmatrix} \cos\theta & -\sin\theta \\ \sin\theta & \cos\theta \end{bmatrix} \begin{bmatrix} V_d \\ V_q \end{bmatrix} \tag{3.10}$$

where V_d and V_q are the synchronous voltage components and V_α, V_β are the stationary reference voltages.

PWM Generation and Inverter Switching: The generated three-phase reference voltages V_{abcref} are supplied to the PWM generator. The PWM module compares these reference signals with a high-frequency carrier waveform to generate gate pulses for the inverter switches. The duty ratio is determined according to

$$D = \frac{V_{ref}}{V_{carrier}} \tag{3.11}$$

where Ddenotes the PWM duty cycle, $V_{ref}$is the reference modulation signal, and $V_{carrier}$is the carrier waveform amplitude. The PWM pulses regulate inverter switching and control bidirectional power transfer.

LCL Filter and Grid Interface: The inverter output current passes through the LCL filter before reaching the utility grid. The filter significantly attenuates switching-frequency harmonics while preserving the fundamental frequency component. The active and reactive powers exchanged with the grid are expressed as

$$P = \frac{3}{2}(V_d I_d + V_q I_q) \tag{3.12}$$

$$Q = \frac{3}{2}(V_q I_d - V_d I_q) \tag{3.13}$$

where Pdenotes active power, Qrepresents reactive power, and V_d, V_q, I_d, and $I_q$are the synchronous voltage and current components.

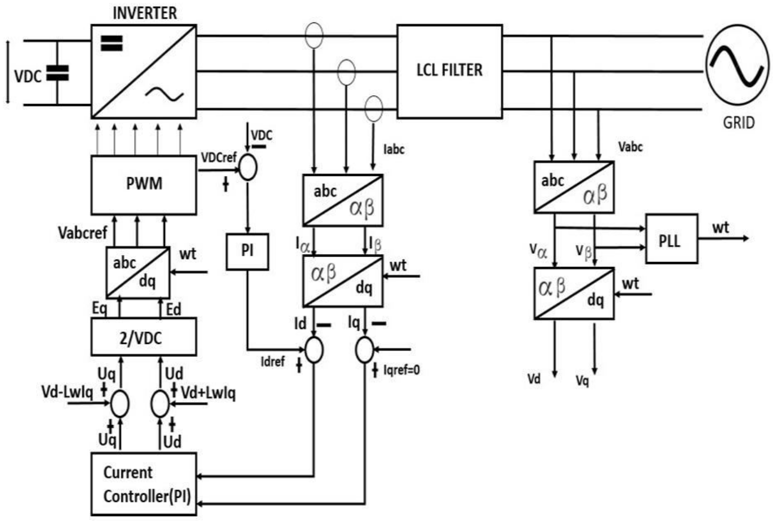

Figure 5. Proposed ANN Control System

The coordinated operation of the PLL, Clarke transformation, Park transformation, ANN DC voltage controller, ANN current controller, PWM generator, inverter, and LCL filter establish a fully adaptive intelligent control strategy for the bidirectional EV charger. The ANN continuously learns the nonlinear behavior of the converter and grid, thereby improving voltage regulation, current tracking accuracy, harmonic suppression, converter efficiency, and dynamic stability during both G2V charging and V2G discharging. Consequently, the proposed ANN-based controller provides faster convergence, reduced steady-state error, enhanced robustness against parameter variations, and superior overall performance compared with conventional PI-based control systems.

4. RESULTS AND DISCUSSION

Figure 6 illustrates the MATLAB/Simulink implementation of the proposed ANN-based bidirectional battery charger for EV applications operating in both G2V and V2G modes. The model consists of a three-phase AC source, voltage and current measurement units, LCL filter, bidirectional AC/DC converter, DC-link capacitor, bidirectional DC/DC converter, battery model, ANN-based voltage controller, ANN-based current controller, dq-axis transformations, PWM generator, and switching circuits. Unlike the existing PI controller, the ANN controller continuously learns the nonlinear relationship between converter inputs and outputs, thereby generating adaptive control signals for the converters.

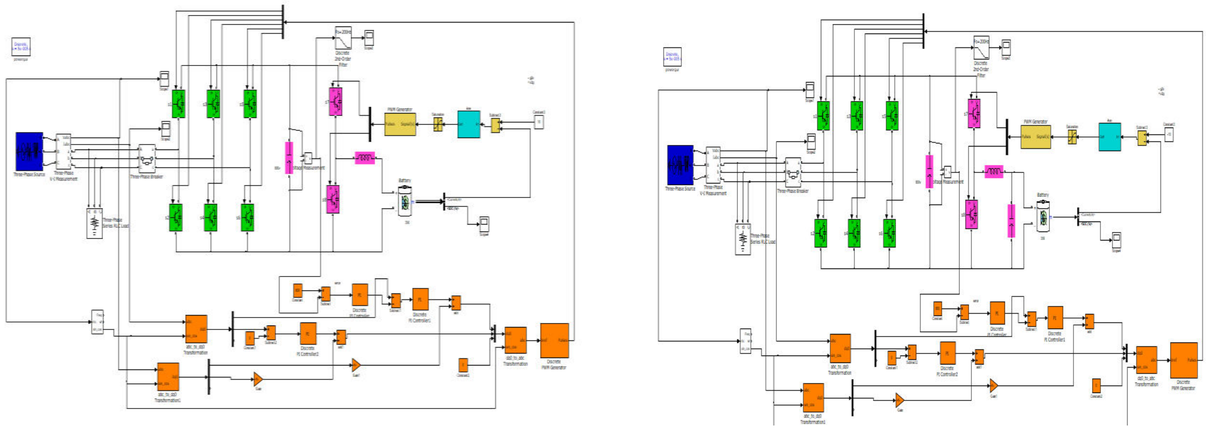

(a) (b)

Figure 6. MATLAB/Simulink Model of the Proposed ANN-Based Bidirectional Battery Charger. (a) G2V. (b) V2G.

The intelligent controller improves DC-link voltage regulation, minimizes steady-state error, enhances converter stability, and reduces harmonic distortion under dynamic operating conditions while maintaining efficient bidirectional power transfer.

Figure 7 presents the DC-link voltage response of the proposed ANN-controlled charger during G2V operation. The voltage rises rapidly from 0 V and reaches a maximum transient value of approximately 825 V, after which it quickly settles at the reference voltage of 800 V. Compared with the conventional PI controller, the ANN controller exhibits lower overshoot and faster settling characteristics, with the voltage becoming stable within approximately 0.006 s. The steady-state voltage remains almost constant at 800 V throughout the remaining simulation interval of 0.1 s, demonstrating excellent voltage regulation and improved dynamic performance.

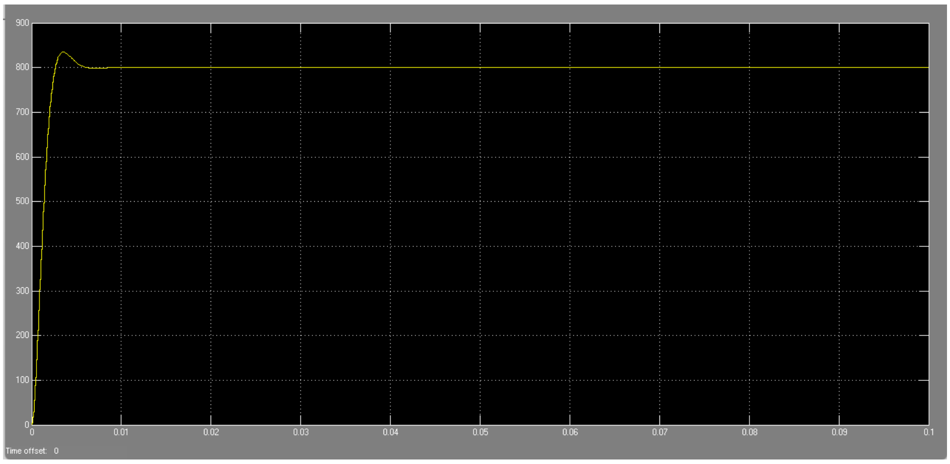

Figure 7. Proposed G2V Mode Output Voltage Response

Figure 8 illustrates the battery SoC variation during Grid-to-Vehicle charging operation using the proposed ANN controller. Initially, the battery SoC is approximately 0.01%, and it gradually increases as charging progresses. At the end of the simulation period (0.1 s), the battery SoC reaches approximately 0.315%, confirming continuous charging of the battery. The charging profile remains smooth without noticeable oscillations, indicating that the ANN controller effectively regulates the charging current while improving battery charging stability and energy utilization.

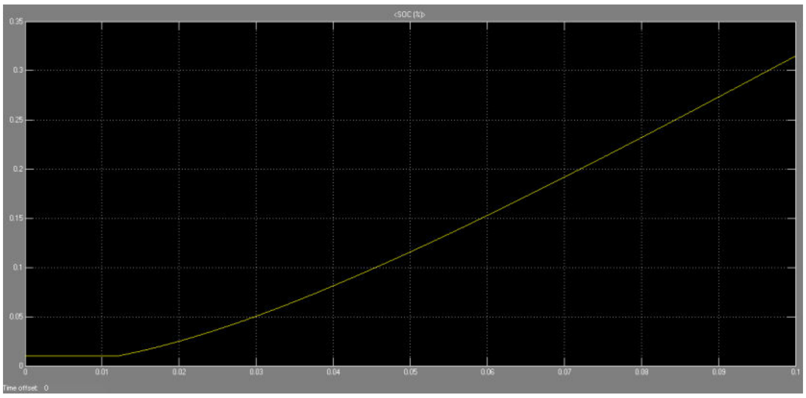

Figure 8. Proposed G2V Battery SoC Characteristics

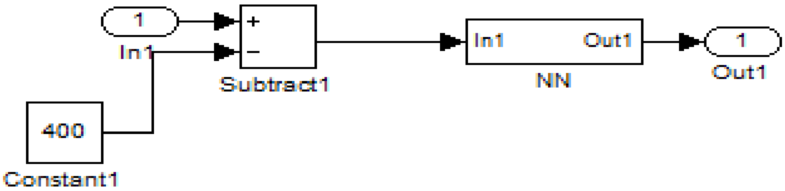

Figure 9. Proposed ANN Controller Structure

Figure 9 illustrates the implementation of the Artificial Neural Network (ANN) controller employed in the proposed bidirectional battery charger. The measured converter output is first compared with the reference value of 400, and the resulting error signal is generated through the subtraction block. This error is supplied as the input to the ANN block, which processes the nonlinear relationship between the reference and measured signals using its trained neural network model. The ANN produces an adaptive control output that replaces the conventional fixed-gain PI controller output. The intelligent controller continuously adjusts converter control signals according to operating conditions, thereby improving voltage regulation, current tracking, dynamic response, and overall converter performance.

Figure 10 presents the Fast Fourier Transform (FFT) analysis of the grid current during Grid-to-Vehicle operation using the proposed ANN controller. The fundamental frequency is maintained at 50 Hz, with a fundamental magnitude of approximately 328 V. The Total Harmonic Distortion (THD) is reduced to 2.00%, which is significantly lower than the 4.21% obtained using the conventional PI controller. The harmonic spectrum shows considerably reduced lower-order harmonic components, confirming that the ANN controller improves current waveform quality, enhances converter efficiency, and satisfies grid harmonic requirements more effectively.

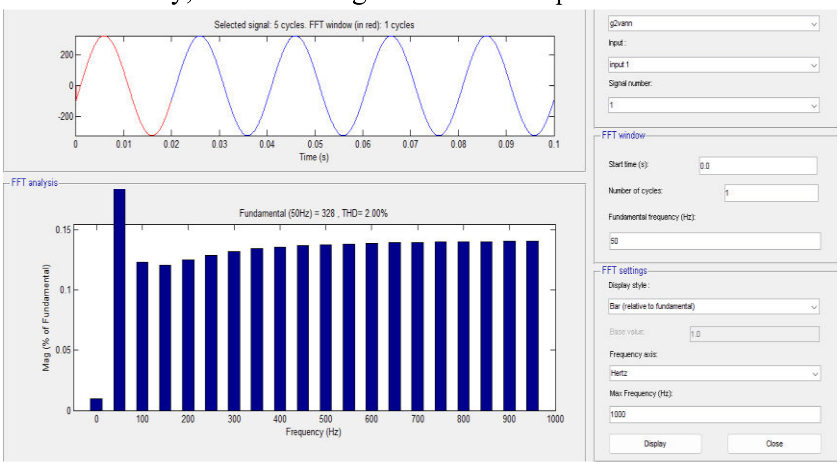

Figure 10. Proposed G2V FFT Analysis.

Figure 11 illustrates the MATLAB/Simulink implementation of the proposed ANN-controlled bidirectional battery charger operating in V2G mode. The model includes the three-phase inverter, LCL filter, bidirectional converters, battery energy storage system, ANN controller, voltage and current measurement units, dq-axis control blocks, and PWM generation circuits. During V2G operation, the battery supplies stored energy back to the utility grid while the ANN controller continuously regulates converter switching to maintain stable DC-link voltage, synchronized grid current, and efficient bidirectional power transfer. The intelligent controller enables rapid adaptation to varying grid conditions and improves overall converter stability.

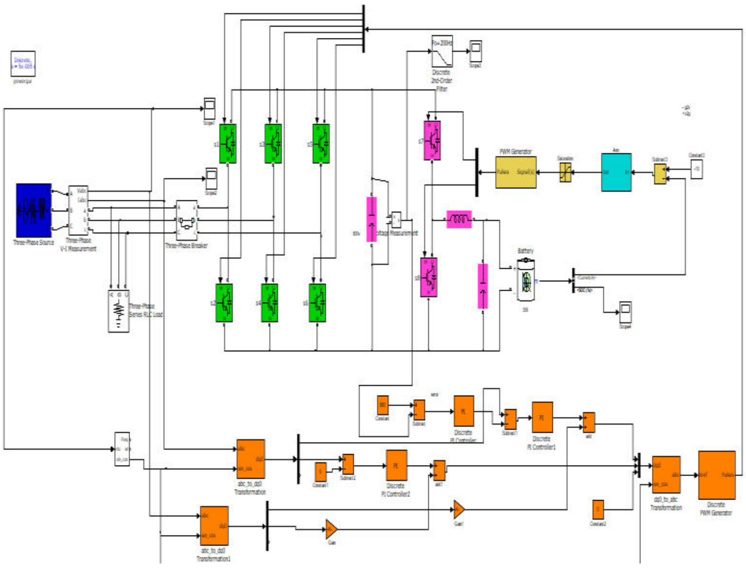

Figure 11. MATLAB/Simulink Model of the Proposed ANN-Based V2G Operation

Figure 12 presents the DC-link voltage response of the proposed ANN controller during Vehicle-to-Grid operation. The output voltage initially increases from 0 V and reaches a transient peak of approximately 825 V before settling to the desired operating voltage of 800 V. The voltage stabilizes within approximately 0.006 s, which is faster than the conventional PI controller. Throughout the simulation interval of 0.1 s, the voltage remains nearly constant without noticeable oscillations, demonstrating the excellent voltage regulation capability of the ANN controller during battery discharging operation.

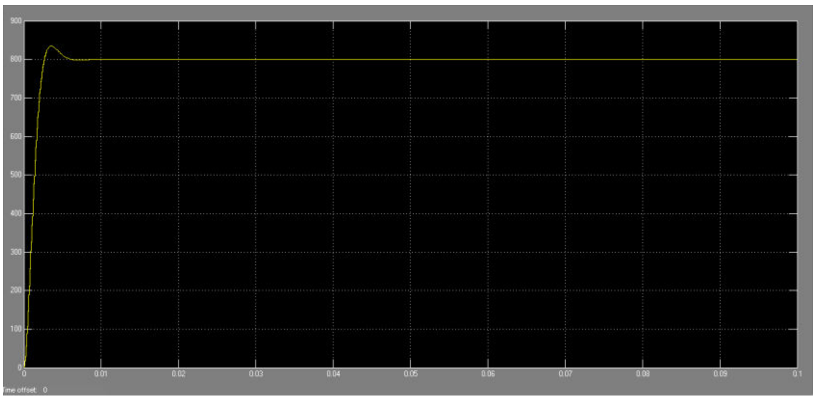

Figure 12. Proposed V2G Mode Output Voltage Response

Figure 13 illustrates the battery State-of-Charge variation during Vehicle-to-Grid operation. The battery initially possesses an SoC of approximately 80.00%, and as electrical energy is supplied to the utility grid, the SoC gradually decreases. At the end of the simulation period, the battery SoC reaches approximately 79.83%, confirming stable and continuous battery discharging. The smooth discharge profile without abrupt fluctuations indicates that the ANN controller accurately regulates battery current while ensuring reliable energy transfer to the grid.

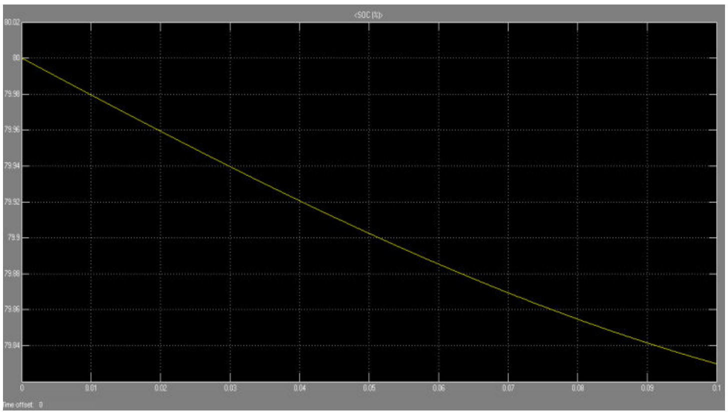

Figure 13. Proposed V2G Battery State-of-Charge Characteristics

Figure 14 presents the ANN controller employed during Vehicle-to-Grid operation. Similar to G2V mode, the measured converter output is compared with the reference value of 400, and the resulting error signal is supplied to the ANN block. The trained neural network processes the input error and generates adaptive control signals that regulate converter switching according to changing battery and grid conditions. This adaptive learning capability enables faster transient response, improved converter stability, enhanced current regulation, and superior overall performance during battery discharging.

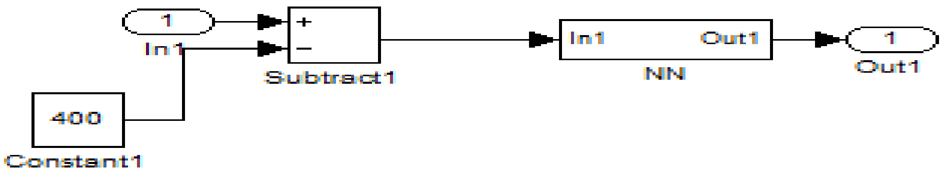

Figure 14. Proposed ANN Controller Structure for V2G Operation

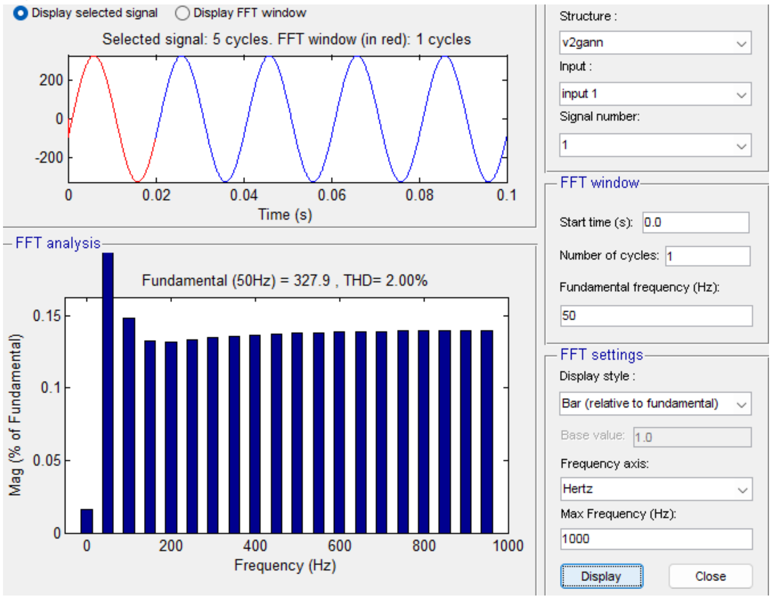

Figure 15. Proposed V2G FFT Analysis

Figure 15 presents the Fast Fourier Transform (FFT) analysis of the proposed ANN-controlled charger during Vehicle-to-Grid operation. The measured fundamental frequency remains at 50 Hz, while the fundamental voltage magnitude is approximately 327.9 V. The Total Harmonic Distortion (THD) is measured as 2.00%, representing a substantial improvement over the 6.00% obtained using the conventional PI controller. The harmonic spectrum exhibits significantly reduced lower-order harmonic amplitudes and improved sinusoidal current characteristics, demonstrating that the ANN controller effectively enhances power quality, minimizes converter harmonics, and provides superior bidirectional energy conversion performance.

4.1 Comparative Analysis

Table 1 compares the harmonic characteristics obtained during Grid-to-Vehicle operation. Both controllers operate at the standard grid frequency of 50 Hz. The proposed ANN controller slightly improves the fundamental voltage while significantly reducing the Total Harmonic Distortion from 4.21% to 2.00%. The lower THD indicates superior harmonic suppression, improved power quality, and enhanced compliance with grid standards.

Table 1. Comparison of G2V Harmonic Performance

Parameter	Existing PI Controller	Proposed ANN Controller
Fundamental Frequency (Hz)	50	50
Fundamental Voltage (V)	324.9	328.0
THD (%)	4.21	2.00
Harmonic Performance	Good	Excellent
Grid Current Quality	Good	Very Good

Table 2 compares the FFT analysis obtained during Vehicle-to-Grid operation. The proposed ANN controller maintains the same grid frequency while improving the fundamental voltage from 323.1 V to 327.9 V. More importantly, the Total Harmonic Distortion decreases substantially from 6.00% to 2.00%, representing nearly a 67% reduction in harmonic distortion. This improvement demonstrates the effectiveness of the ANN controller in producing cleaner current waveforms and enhancing grid power quality during battery discharging.

Table 2. Comparison of V2G Harmonic Performance

Parameter	Existing PI Controller	Proposed ANN Controller
Fundamental Frequency (Hz)	50	50
Fundamental Voltage (V)	323.1	327.9
THD (%)	6.00	2.00
Harmonic Performance	Moderate	Excellent
Grid Current Quality	Good	Excellent

5. CONCLUSION

The proposed ANN-based bidirectional battery charger demonstrated superior performance over the conventional PI controller for both Grid-to-Vehicle (G2V) and Vehicle-to-Grid (V2G) operations. The ANN controller achieved faster dynamic response, reduced voltage overshoot, improved DC-link voltage regulation, and significantly lowered total harmonic distortion (THD) during both charging and discharging modes. It also enhanced battery charging and discharging control, converter stability, power quality, power factor, and overall converter efficiency while eliminating the need for repeated manual controller tuning. The integration of adaptive ANN control with bidirectional converters and an LCL filter enabled reliable bidirectional power transfer under varying grid and battery conditions. Future work will focus on incorporating deep learning and reinforcement learning techniques, real-time DSP/FPGA implementation, renewable energy integration, battery health monitoring, and cybersecurity mechanisms to further improve the intelligence and reliability of EV charging systems.

REFERENCES

[1]. J. G. Pinto, V. Monteiro, H. Gonçalves, B. Exposto, C. Couto, and João L. Afonso, "Bidirectional battery charger with Grid-to-Vehicle, Vehicle-to-Grid and Vehicle-to-Home

technologies," in Proceedings of the 39th Annual Conference of the IEEE Industrial Electronics Society (IECON 2013), Vienna, Austria, Nov. 2013, pp. 5934–5939, doi: 10.1109/IECON.2013.6700108.

[2]. R. Zgheib, K. Al-Haddad and I. Kamwa, "V2G, G2V and active filter operation of a bidirectional battery charger for electric vehicles," 2016 IEEE International Conference on Industrial Technology (ICIT), Taipei, Taiwan, 2016, pp. 1260-1265, doi: 10.1109/ICIT.2016.7474935.

[3].] Chakraborty, S., Vu, H.N., Hasan, M.M., Tran, D.D., Baghdadi, M.E. and Hegazy, O., 2019. DC-DC converter topologies for electric vehicles, plug-in hybrid electric vehicles and fast charging stations: State of the art and future trends. Energies, 12(8), p.1569.

[4]. B. Koushki, A. Safaee, P. Jain and A. Bakhshai, "Review and comparison of bi-directional AC-DC converters with V2G capability for on-board EV and HEV," 2014 IEEE Transportation Electrification Conference and Expo (ITEC), Dearborn, MI, USA, 2014, pp. 1-6, doi: 10.1109/ITEC.2014.6861779.

[5]. V. K, R. K. Nema and A. Ojha, "Various Types of Wireless Battery Management System in Ev," 2020 IEEE International Students' Conference on Electrical,Electronics and Computer Science. Restrictions apply. (SCEECS), Bhopal, India, 2020, pp. 1-5, doi: 10.1109/SCEECS48394.2020.115.

[6]. Kumar, M., Ojha, A. (2022). Design Consideration for e-Rikshaw with Regeneration Capability. In: Verma, P., Samuel, O.D., Verma, T.N., Dwivedi, G. (eds) Advancement in Materials, Manufacturing and Energy Engineering, Vol. I. Lecture Notes in Mechanical Engineering. Springer, Singapore. https://doi.org/10.1007/978-981- 16-5371-1_15.

[7]. Kumar, M. and Ojha, A., 2019. Key developments for electric vehicles in local transport. J Instrum Inno Sci, 4(2), pp.36-45.

[8]. Ojha, A., Chaturvedi, P., Mittal, A. and Jain, S., 2016. Carrier based common mode voltage reduction techniques in neutral point clamped inverter-based AC-DC-AC drive system. Journal of Power Electronics, 16(1), pp.142-152.

[9]. Viswanatha, V., Ramachandra, A.C. & Venkata Siva Reddy, R. Bidirectional DC-DC converter circuits and smart control algorithms: a review. Journal of Electrical Systems and Inf Technol 9, 6 (2022). https://doi.org/10.1186/s43067-022- 00048-z.

[10]. Viswanatha V, Venkata Siva Reddy R, Rajeswari (2020) Research on state space modeling, stability analysis and PID/PIDN Control of DC–DC converter for digital implementation. In: Sengodan T., Murugappan M., Misra S. (eds) Advances in Electrical and Computer Technologies. Lecture Notes in Electrical Engineering, 672: 1255–1272.

[11]. Ashwini Kumari P, Geethanjali P (2018) Parameter estimation for photovoltaic system undernormal and partial shading conditions. A survey. Renew Sustain Energy Rev 84:1–11

[12]. Dominguez X, Camacho O, Leica P, Rosales A (2016) A fixed-frequency Sliding-mode control in a cascade scheme for the Half-bridge Bidirectional DC-DC converter. Proc. IEEE ETCM, 2016, Guayaquil, pp. 1–6.

[13]. Tahim, A.P.N. ; Pagano, D.J. ; Ponce, E., "“Nonlinear control of dc-dc bidirectional converters in stand-alone dc Microgrids ”," in Decision and Control (CDC), 2012 IEEE 51st Annual Conference on, vol., no., pp. 3068–3073, 10-13 Dec. 2012.

[14]. A. Aravkin, J. Burke, A. Chiuso, and G. Pillonetto. On the estimation of hyperparameters for empirical Bayes estimators: Maximum marginal likelihood vs minimum MSE. In Proceedings of IFAC SYSID, 2012.